Maxar's WorldView-3 Enables Low-Concentration Methane Detection from Space

Andreas Hayden[(1)], Joseph Christy[(2)]

(1) Corresponding author, Maxar Technologies; andreas.hayden@maxar.com

(2) Maxar Technologies

Abstract

Methane is large contributor to climate change; for this reason, detecting and eliminating sources of methane emissions is a key element to minimizing the effects of on-going climate change. While there are a variety of methods currently used to detect methane emissions, ranging from ground-based sensors to aerial sensors like drones and aircraft, satellite detections provide a broad-area coverage addition to these other methods. Satellites are ideally situated to perform detections worldwide and continually monitor areas of concern.

In this paper, we present our WorldView-3 results from the 2022 Stanford Controlled Methane Release Experiment and describe how this experiment enabled us to uncover a misinterpretation of our spectral data Base. In the single blind, controlled release experiment, our detection algorithms using Maxar's WorldView-3 satellite and its shortwave infrared (SWIR) sensor was able to correctly detect and quantify emissions down to 33 kg per hour (kg/hr). The Stanford experiment was so well designed and executed that we quickly determined that our mass flow-rate (MFR) estimation included a factor of approximately 2, which was the result of misinterpreting the Pacific Northwest National Laboratory (PNNL) spectral database as Napierian absorbance rather than decadic. Once we uncovered and corrected this misinterpretation, our MFR aligned with the ground truth data.

Key Findings

As a result of our participation in the 2022 Stanford Controlled Methane Release Experiment, we have two key findings to report:

1. We found that our detection algorithms using the WorldView-3 satellite was able to correctly detect and quantify emissions down to 33 kg/hr. This detection and quantification were under very good conditions including a low Clutter-Equivalent-Quantity (CEQ) and low wind conditions.
2. We also found that we had assumed the PNNL Quantitative Infrared Database (Sharpe, 2004) was Napierian and therefore our absorbance cross sections were a factor 2.303 too low. Since our baseline cross-sections were a factor of 2.303 too low, our estimates of gas amount in a pixel were a factor of 2.303 high (since it would seem to take more gas in a pixel to achieve the measured spectral absorption). This finding enabled us to correct our spectral database, which in turn made our MFR estimates closely match the ground truth results.

Introduction

Methane, a greenhouse gas, is a strong contributor to climate change. Detecting and stopping methane leaks is an important tool in combatting climate change (Than, 2016).

Maxar participated in the 2022 Controlled Methane Release Experiment run by Stanford University by providing spectral imagery from the WorldView-3 satellite and analysis detecting and quantifying methane plumes in the imagery. The experiment was a continuation of Stanford's 2021 study (Sherwin, 2023). WorldView-3's 3.7 m ground sample distance (GSD) in SWIR imagery allowed for detection of methane down to metered release rates of 33 kg/hr.

Maxar's WorldView-3 satellite provides a unique contribution to the current suite of satellites (Jacob, 2022), both currently in orbit and planned, that are monitoring methane leaks around the world. WorldView-3 is a multispectral imaging satellite with 29 spectral bands ranging from 0.4μ to 2.5μ and the capacity to image 680,000 square kilometer (sq km) per day. While WorldView-3 was not designed as a methane detector, six of the eight SWIR bands overlap with methane absorption features (Figure 1). The additional visible and near infrared (NIR) bands provide additional spectral and image information to help identify sources of fugitive methane. Furthermore, the small GSD in WorldView-3's SWIR imagery increases sensitivity to detecting point sources of methane.
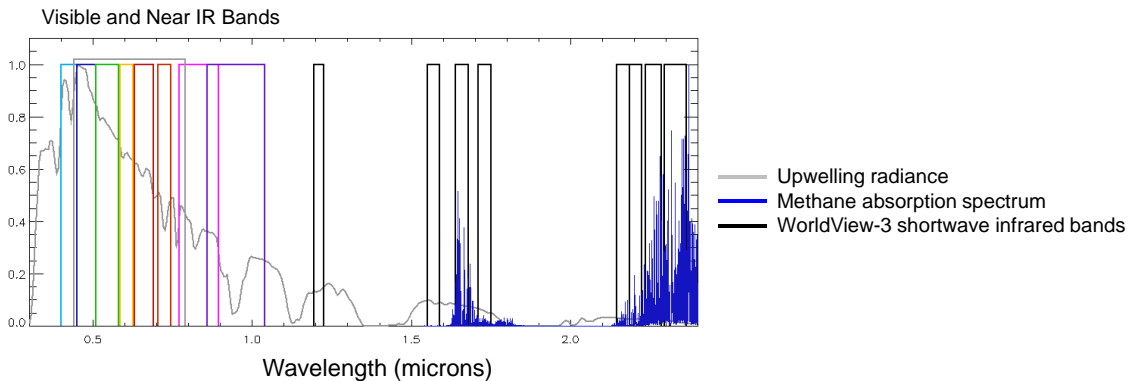

Figure 1. Wavelengths of WorldView-3 visible, near infrared (IR) and shortwave IR bands include key portions of the methane absorption spectrum. The y-axis units are arbitrary. All plots are scaled to a peak value of one.

Earlier work using WorldView-3 SWIR imagery (Sanchez-Garcia, 2022) has shown point source methane leaks down to 30 kg/hr but the data lacked ground truth.

In addition to verifying detectability of low release rates, because of a well-executed experiment and good ground control data, we uncovered a factor-of-2 misinterpretation of our spectral database resulting in a 2X error in our MFR estimates.

In the following sections, we will discuss sensitivity to GSD, the factor-of-2 error, and the detection and quantification results of our analysis of the Stanford controlled release data.

Dependency of Gas Detectable Quantity on Pixel Size

Detection and quantification of methane from satellite imagery depends on a number of factors including the emission rate, local wind speed, GSD, and cloud cover. For a given point source MFR and wind speed; a small pixel size decreases the minimum detectable MFR in a pixel. Equation1 shows, via basic geometry, that MFR estimate is a product of GSD, wind speed and the methane concentration.

$$MFR = GSD \times u_w \times \Delta XCH_4$$

Equation 1

MFR: mass flow-rate estimate (molecules/second)
GSD: ground sample distance (m)
u_w: wind speed (m/second)
ΔXCH₄: methane column depth (molecules/sq m)

WorldView-3's 3.7 m GSD in the SWIR bands enable sensitivity to discover sources of methane approaching that of hyperspectral instruments with large GSD. Note however, since WorldView-3 is a multispectral imager, it does not have the ability to discriminate among gasses with similar spectral features (such as methane, propane, and ethane) that hyperspectral instruments can.

Factor of 2.303 Error in Interpreting the PNNL Spectral Database

One fortuitous result of this study is that we found that our interpretation of the PNNL Spectral Database we had been using for methane absorption was a factor of 2.303 low. Estimating the amount of methane contained in a multispectral image pixel relies on comparing the depth of an absorption line to a calibrated spectral cross-section (Beer's Law). Any error in spectral cross-section translates directly to an error in estimated gas amount. Estimating MFR, in turn, depends on accurately estimating the amount of gas in the area defined by a pixel in a spectral image.

After supplying our MFR estimates to the Stanford team and then receiving the ground truth estimates, we found our MFR estimates to be consistently approximately a factor of 2 high. The problem was traced to the database of spectral absorption cross-sections we had been using.

Our baseline spectral database, used for our original submission, was the PNNL Database for Quantitative Infrared Spectroscopy. When compared to an independent database, QASoft Library by Hanst Infrared Analysis Inc, we recognized that our interpretation of the PNNL absorption cross-section is low (Figure 2).
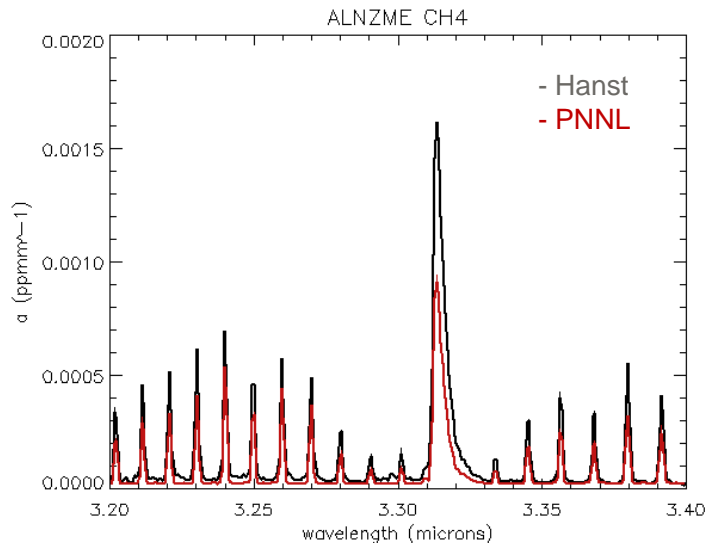

Figure 2. This comparison of the Hanst and the PNNL methane absorption curves reveals the factor-of-2 error.

The Hanst database however does not contain data in the 2.3μ region required for methane quantification. So, a further investigation was performed using the MODTRAN radiative transfer code (Berk, 2014). An atmospheric path with a known amount of methane was modeled and the methane cross-section was estimated via the MODTRAN-generated path transmission and Beer's law. Figure 3 shows the comparison between MODTRAN results and the PNNL database. Again, the PNNL spectrum is low.
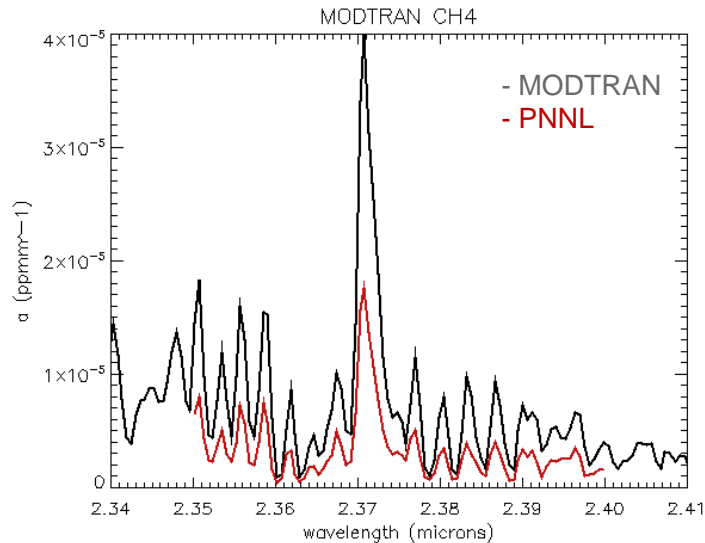

Figure 3. This comparison of the MODTRAN and the PNNL methane absorption curves reveals the factor-of-2 error.

Since our baseline database cross-sections where approximately a factor-of-2 low, our estimates of gas quantity in a pixel where a factor-of-2 high (since it would seem to take twice as much gas in a pixel to achieve the measured spectral absorption). The results in the following sections use the corrected interpretation of the spectral database.

WorldView-3 Methane Detection and Quantification Results

In October and November of 2022, Maxar participated in a controlled methane release experiment run by Stanford University similar to their test in 2021 (Sherwin, 2023). For the test, Stanford released measured amounts of methane for the short time the methane plume was within view of the overhead sensors. The MFR estimate tests were run in several stages. Participants would collect imagery of the release site during controlled releases. Initially, teams would have access to neither locally collected wind data nor to methane release rates (blind wind speed, blind MFR). Participants sent their MFR estimates to Stanford, and then Stanford shared locally measured wind information (unblind wind) and allowed a second set of MFR estimates to be submitted. This paper focuses on results from this second round of MFR estimates (unblind wind, blind MFR) using data collected from Maxar's WorldView-3 satellite.

In this paper, MFR estimates were based on the Integrated Mass Enhancement (IME) method (Varon, 2018). For the data presented here, the wind speed used in the IME equation is the ground truth wind speed measured at the methane release site, and the plume length used is the length of the long axis of the detected plume. The integrated methane mass is the gas quantity measured in the methane quantity image in the pixels in the detected plume. Figure 4 outlines the parts feeding the IME equation.
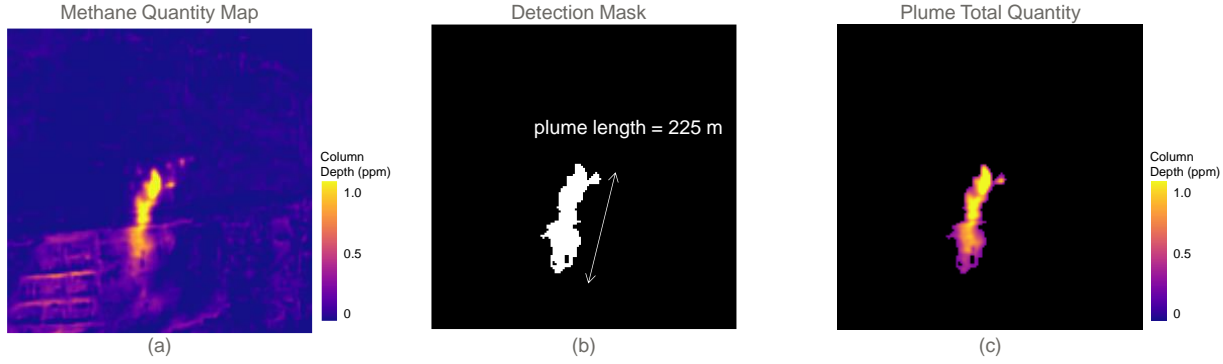
Figure 4. Contributors to MFR estimate using IME. (a) methane quantity map (CEQ=0.08 parts per million [ppm]), (b) pixels above clutter level (detection mask), (c) sum of methane quantity in detection mask.

Due to the variable reflectivity in a spectral scene, there is a variability in detected methane even when no methane is present. The standard deviation of this background detected methane is referred to as the Clutter-Equivalent-Quantity (CEQ) and is measured in units of column depth. The uncertainty in MFR presented below arises from the variability of the wind speed during the data collect and the scene CEQ.

Table 1 below summarizes our results from WorldView-3 imagery (post unblind wind and one case of post unblind MFR). In general, our lowest true-positive MFR was 33 kg/hr, we found no false-positives, and we have one false negative (10/17/2022).

Table 1. Estimated and ground truth MFR for controlled release experiments using updated spectral database.

Image Name	Collection date	Ground Truth			Maxar Estimate		Comment
		wind speed (m/s)	+/- (m/s)	MFR (kg/hr)	MFR (kg/hr)	+/- (kg/hr)	
22OCT10181729	10/10/2022	0.94	0.24	93	46	13	known wind
22OCT17182742	10/17/2022	1.87	0.39	40	42	13	known wind, known MFR
22OCT29181742	10/29/2022	1.34	0.42	33	34	13	known wind
22NOV05182744	11/05/2022	0.46	0.14	0	0	11	known wind
22NOV10180843	11/10/2022	2.13	0.52	1106	1135	278	known wind
22NOV17181847	11/17/2022	5.67	0.70	601	602	78	known wind
22NOV22175839	11/22/2022	0.90	0.36	433	240	96	known wind
22NOV24182859	11/24/2022	6.74	0.74	0	0	149	known wind
22NOV29180846	11/29/2022	4.31	0.73	1315	1371	233	known wind

Compare Estimated MFR to Ground Truth

Figure 5 summarizes the results of estimating MFR using WorldView-3 SWIR imagery. Once the factor of 2.303 in our spectral database is accounted for, and knowing the local wind speed, there is good agreement between metered and estimated MFR.
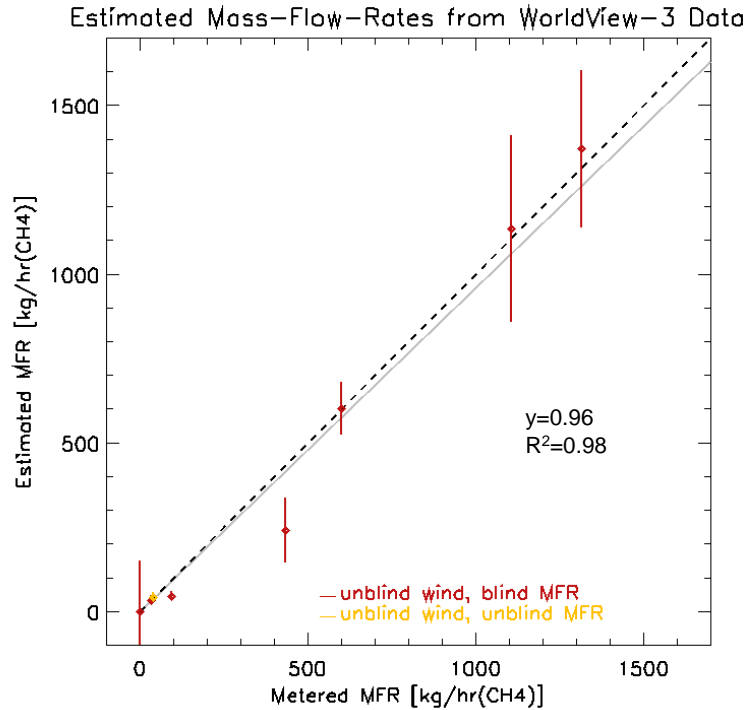
Figure 5. Quantification performance of methane emissions from WorldView-3 data. Metered MFR-rate shows good agreement with single blind and the single fully unblind MFR estimation results.

The solid grey line is a linear fit with intercept fixed at zero, the slope (y) and centered R^2 are displayed. The black dashed line is the perfect 1:1 line.

Known Wind, Blind MFR

The following eight figures show methane concentration measured from the WorldView-3 satellite for eight of the nine controlled releases in the study. Metered release rates varied from 0 kg/hr to approximately 1300 kg/hr. These represent the six true detects and two true negatives our team identified. The false negative result is discussed in the next section.

The base images in eight of the nine the following figures are pan-sharpened, natural color images uploaded from Maxar's SecureWatch platform. The panchromatic image and visible images used to make the pan-sharpened, natural color image were collected by WorldView-3 at the same time as the SWIR images used in methane detection and quantification. On November 22, 2022, the skies were reported to be 85% cloud covered, so the pan-sharpened image is not included in SecureWatch. Therefore, the base image for November 22, 2022, is simply WorldView-3 multispectral bands 5, 3, 2 (red, green, blue). The fact that methane was detected below clouds highlights the cloud penetrating ability of SWIR bands. The color scale for all quantity maps is 0 to 1 ppm.

Having the coincident visible spectral image provides context, helping pinpoint the leak location. Also, having the additional spectral information can be used to increase sensitivity, and provides a method to mitigate false alarms by identifying known confusers such as asphalt, paint, and bare soil.
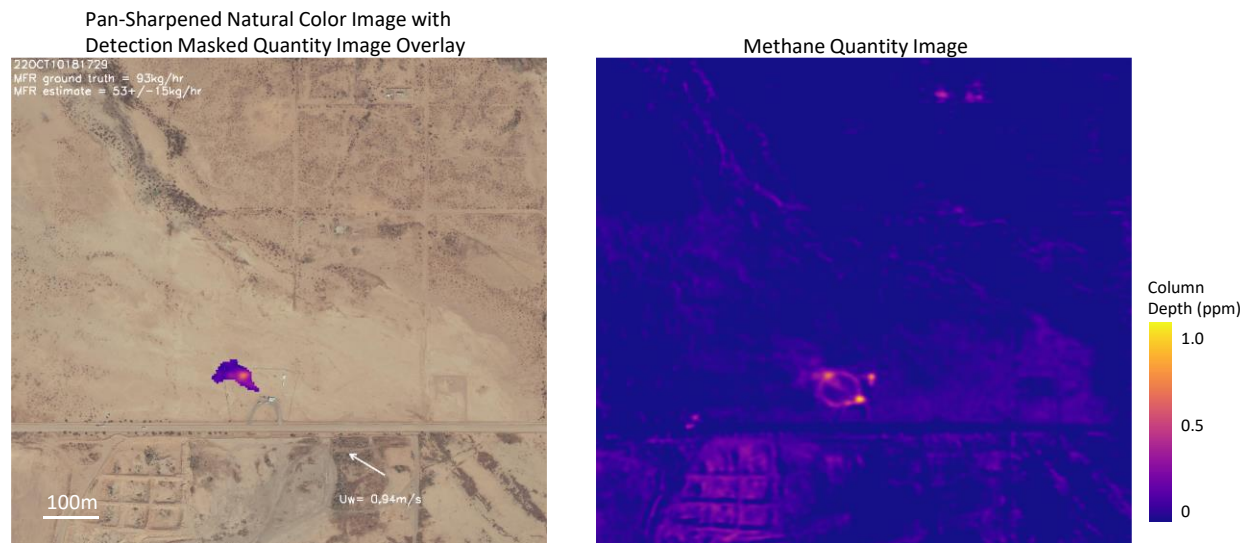
Pan-Sharpened Natural Color Image with
Detection Masked Quantity Image Overlay

Methane Quantity Image

Figure 6. Methane quantity image from October 10, 2022. Ground truth MFR: 93 kg/hr.

Pan-Sharpened Natural Color Image with
Detection Masked Quantity Image Overlay

Methane Quantity Image
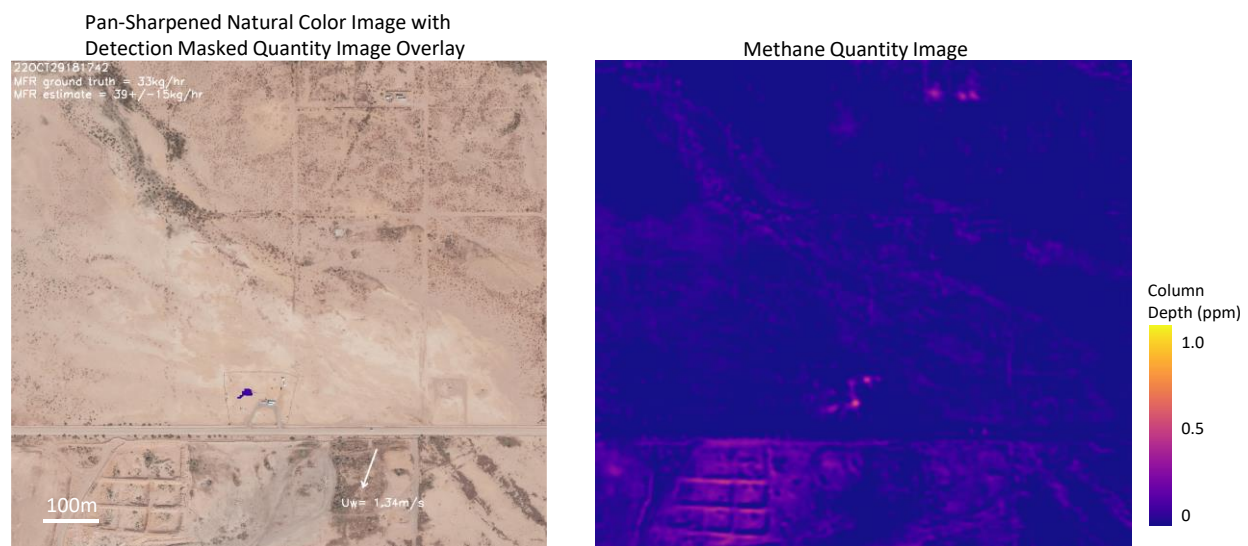
Figure 7. Methane quantity image from October 29, 2022. Ground truth MFR: 33 kg/hr.

Pan-Sharpened Natural Color Image with
Detection Masked Quantity Image Overlay

Methane Quantity Image

22NOV05182744
MFR ground truth = 0kg/hr
MFR estimate = 0+/-13kg/hr

100m

Uw= 0,46m/s

Column
Depth (ppm)

1.0

0.5

0
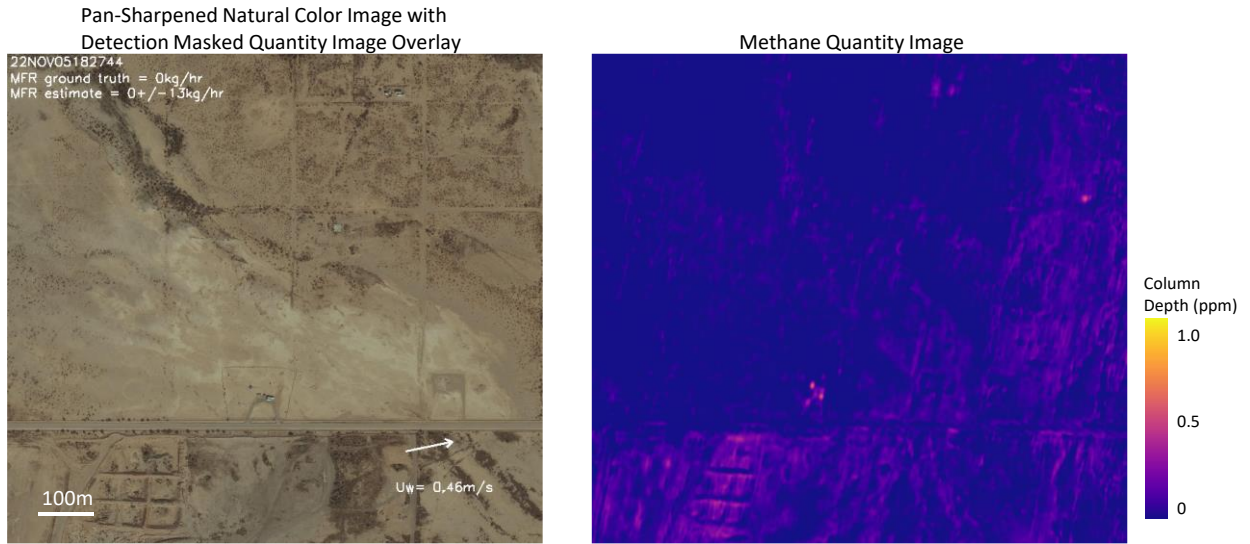
Figure 8. Methane quantity image from November 5, 2022. Ground truth MFR: 0 kg/hr.

Pan-Sharpened Natural Color Image with
Detection Masked Quantity Image Overlay

Methane Quantity Image

22NOV10180843
MFR ground truth = 1106kg/hr
MFR estimate = 1307+/-320kg/hr

100m

Uw= 2,13m/s

Column
Depth (ppm)

1.0

0.5

0
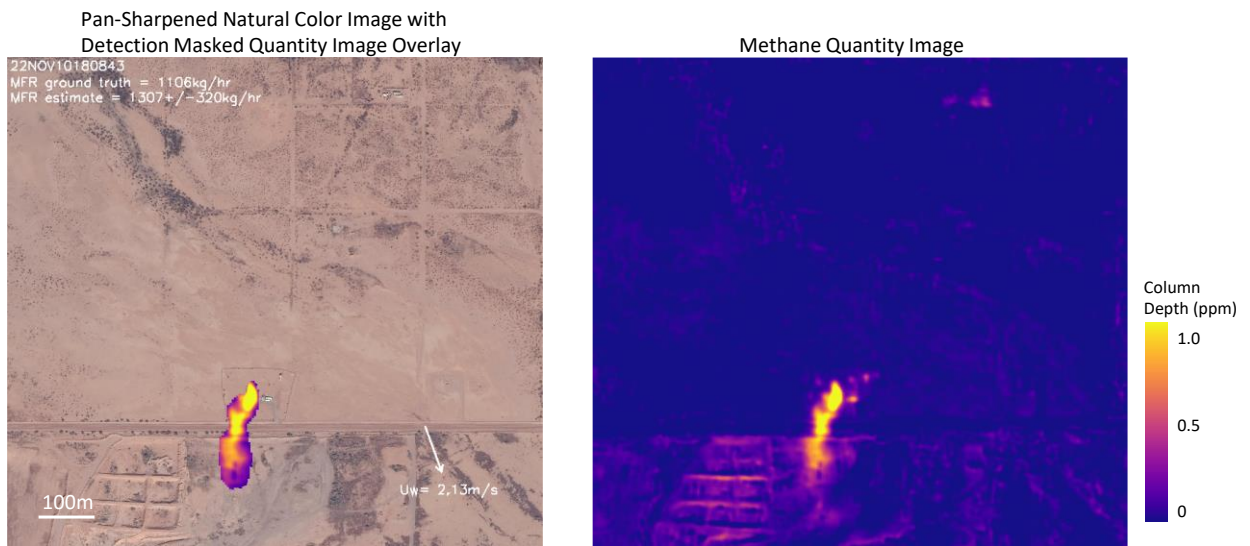
Figure 9. Methane quantity image from November 10, 2022. Ground truth MFR: 1106 kg/hr.

Pan-Sharpened Natural Color Image with
Detection Masked Quantity Image Overlay

Methane Quantity Image
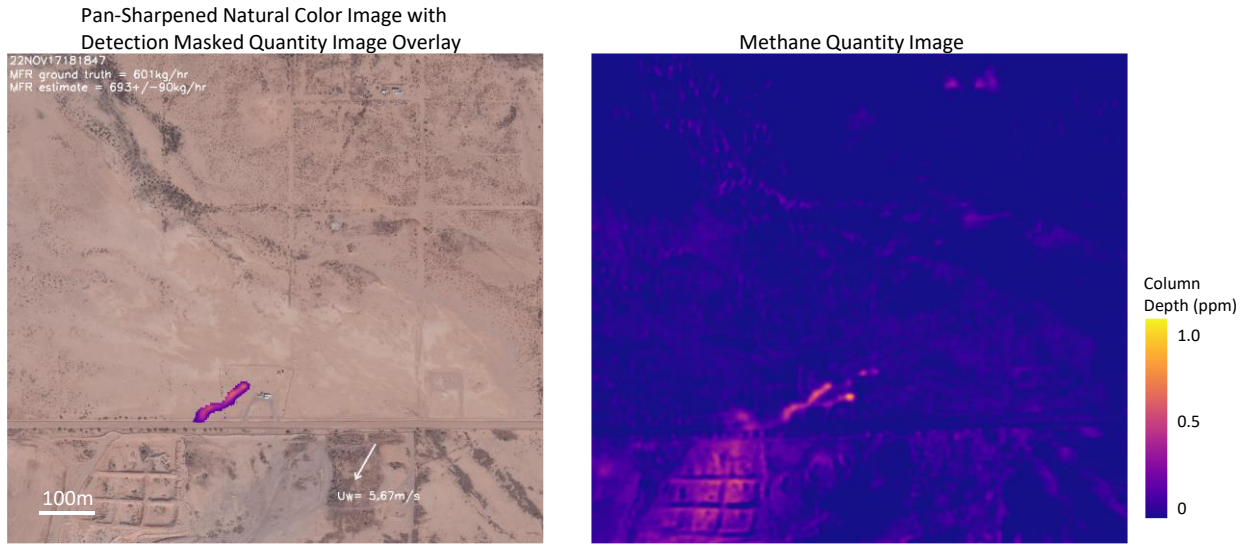
Figure 10. Methane quantity image from November 17, 2022. Ground truth MFR: 601 kg/hr.

RGB Multispectral Color Image with Detection
Masked Quantity Image Overlay

Methane Quantity Image
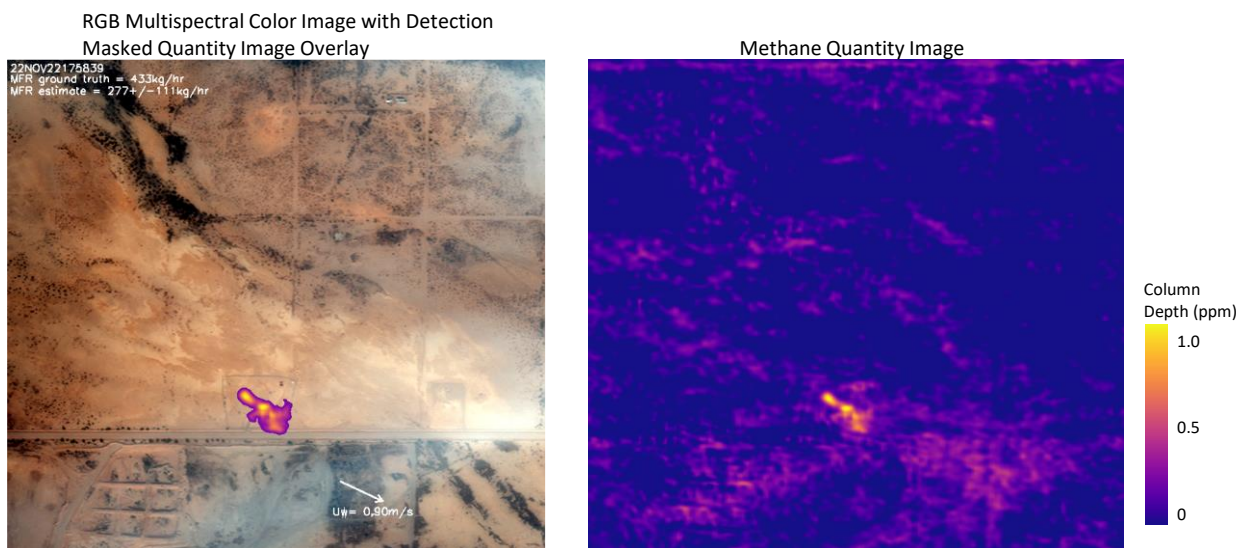
Figure 11. Methane quantity image from November 22, 2022. Ground truth MFR: 433 kg/hr.

Pan-Sharpened Natural Color Image with
Detection Masked Quantity Image Overlay

Methane Quantity Image
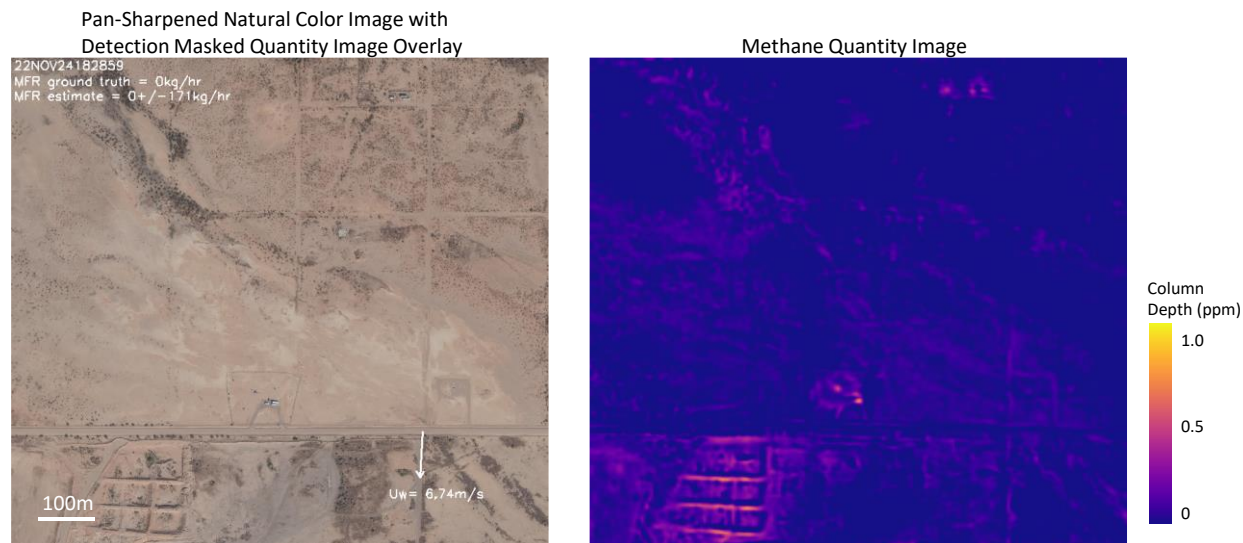
Figure 12. Methane quantity image from November 24, 2022. Ground truth MFR: 0 kg/hr.

Pan-Sharpened Natural Color Image with
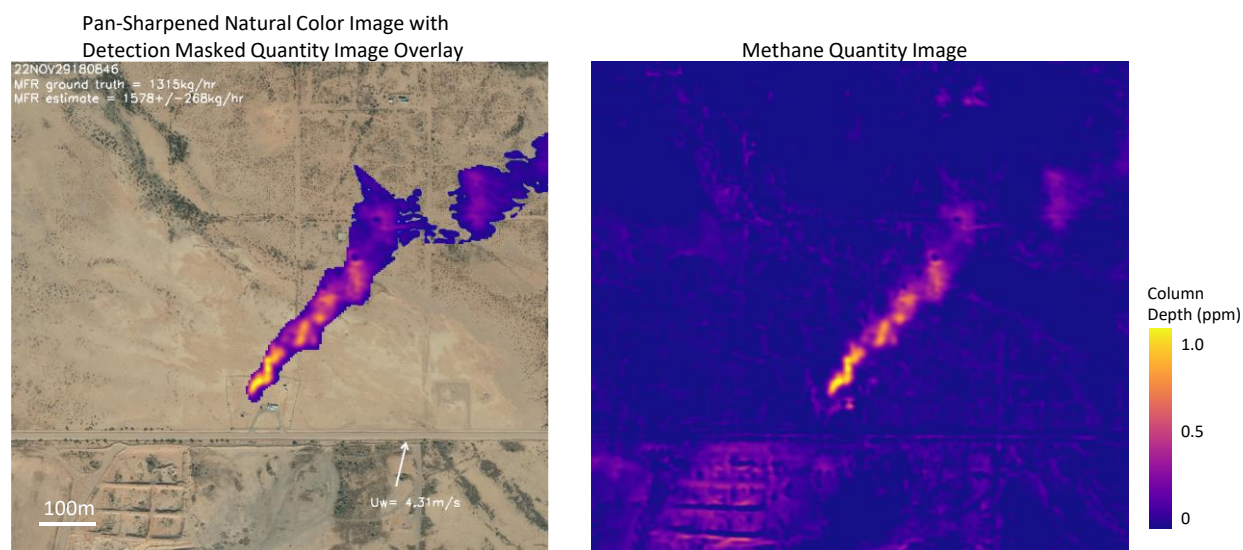Detection Masked Quantity Image Overlay

Methane Quantity Image

Figure 13*. Methane quantity image from November 29, 2022. Ground truth MFR: 1315 kg/hr.*

Known Wind, Known MFR

After providing our results to the Stanford team, we found that we had one false negative. Returning to the image with an improved image processing technique, knowing that there was a release and its location, and knowing the wind direction, a plume can be discerned. We are including estimated release rate for this case as an additional data point to test using the updated PNNL spectral database.
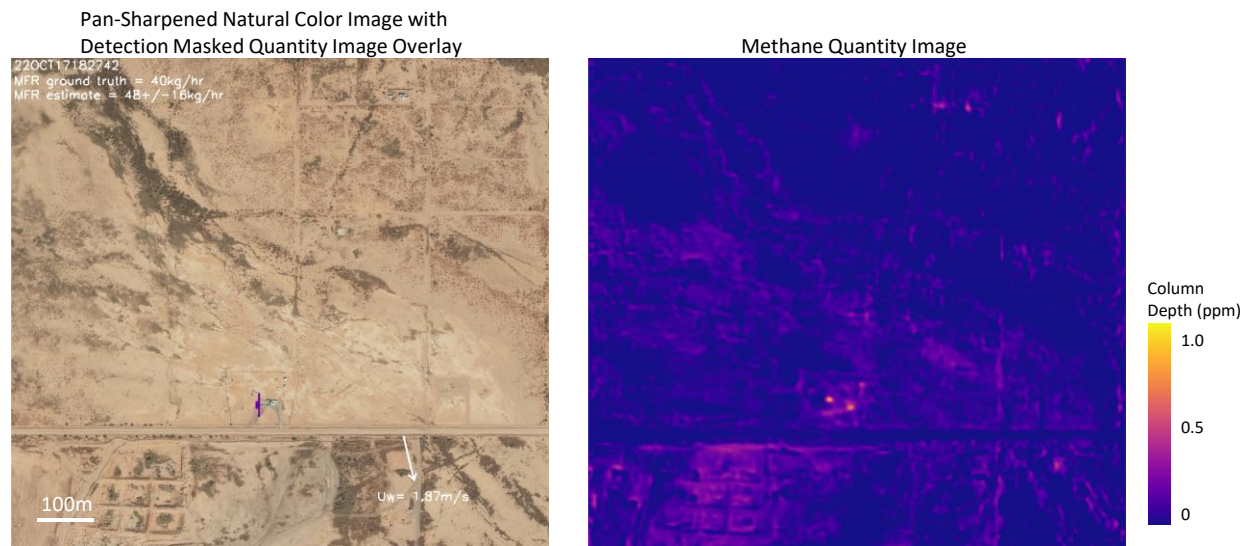
Pan-Sharpened Natural Color Image with
Detection Masked Quantity Image Overlay

Methane Quantity Image

Figure 14. Methane quantity image from October 17, 2022 (post-MFR unblind). Ground truth MFR: 40 kg/hr.

Conclusion

We are very happy to have participated in the 2022 Stanford Controlled Methane Release study. As a result of our participation, and of the care with which Stanford ran the experiment, we uncovered an error in our interpretation of the PNNL database of spectral signatures we were using. More importantly, this study enabled us to further test the capability of the spectral imaging satellites, WorldView-3 in particular, to detect and quantify a variety of methane emission rates, including rates as low as 33 kg/hr.

Acknowledgements

References

Berk, Alexander,Conforti, Patrick,Kennett, Rosemary,Perkins, Timothy,Hawes, Frederick,van den Bosch, Jeannette, "MODTRAN6: a major upgrade of the MODTRAN radiative transfer code",Proc.SPIE 9088, Algorithms and Technologies for Multispectral, Hyperspectral, and Ultraspectral Imagery XX, 2014/6/13, https://doi.org/10.1117/12.2050433

Jacob, D. J.,Varon, D. J.,Cusworth, D. H.,Dennison, P. E.,Frankenberg, C.,Gautam, R.,Guanter, L.,Kelley, J.,McKeever, J.,Ott, L. E.,Poulter, B.,Qu, Z.,Thorpe, A. K.,Worden, J. R.,Duren, R. M., "Quantifying methane emissions from the global scale down to point sources using satellite observations of atmospheric methane",Atmos. Chem. Phys., 22, 14, 2022/07/29, 9617-9646, https://acp.copernicus.org/articles/22/9617/2022/, https://doi.org/10.5194/acp-22-9617-2022

Sánchez-García, E.,Gorroño, J.,Irakulis-Loitxate, I.,Varon, D. J.,Guanter, L., "Mapping methane plumes at very high spatial resolution with the WorldView-3 satellite",Atmos. Meas. Tech., 15, 6, 2022/03/21, 1657-1674, https://amt.copernicus.org/articles/15/1657/2022/, https://doi.org/10.5194/amt-15-1657-2022

Sharpe, Steven W.,Johnson, Timothy J.,Sams, Robert L.,Chu, Pamela M.,Rhoderick, George C.,Johnson, Patricia A., "Gas-Phase Databases for Quantitative Infrared Spectroscopy",Appl Spectrosc, 58, 12, 2004/12/01, 1452-1461, https://doi.org/10.1366/0003702042641281

Sherwin, Evan D.,Rutherford, Jeffrey S.,Chen, Yuanlei,Aminfard, Sam,Kort, Eric A.,Jackson, Robert B.,Brandt, Adam R., "Single-blind validation of space-based point-source detection and quantification of onshore methane emissions",Scientific Reports, 13, 1, 2023/03/07, 3836-3836, https://doi.org/10.1038/s41598-023-30761-2

Than, Ker, (2016) 'Stanford study finds that 'super emitters' are responsible for more than half of U.S. methane emissions'. https://news.stanford.edu/2016/10/26/super-emitters-responsible-bulk-u-s-methane-emissions/

Varon, D. J.,Jacob, D. J.,McKeever, J.,Jervis, D.,Durak, B. O. A.,Xia, Y.,Huang, Y., "Quantifying methane point sources from fine-scale satellite observations of atmospheric methane plumes",Atmos. Meas. Tech., 11, 10, 2018/10/18, 5673-5686, https://amt.copernicus.org/articles/11/5673/2018/, https://doi.org/10.5194/amt-11-5673-2018